AJNR

MR appearance of the internal architecture of Ammon's horn.

M J Miller, L P Mark, K C Ho and V M Haughton

AJNR Am J Neuroradiol 1996, 17 (1) 23-26
http://www.ajnr.org/content/17/1/23

MR Appearance of the Internal Architecture of Ammon's Horn

Marc J. Miller, Leighton P. Mark, Khang-Cheng Ho, and Victor M. Haughton

PURPOSE: To determine whether the four subdivisions of Ammon's horn and six layers of CA1 seen histologically can be demonstrated with MR imaging. **METHODS:** Specimens of cadaver brains were imaged in a 3.0-T MR imager with a 3.0-cm solenoid coil. The specimens were sectioned, stained, and examined histologically. On anatomic sections, the four subdivisions of Ammon's horn and six layers of CA1 were identified. The MR images were then compared with the anatomic sections. **RESULTS:** Using geographic characteristics, we identified the four subdivisions of Ammon's horn. In CA1, the six layers could be identified by variations in signal intensity, width, and location. **CONCLUSION:** This study suggests that, with MR imaging of sufficiently high resolution, the internal architecture of Ammon's horn may be identified.

Index terms: Hippocampus; Brain, anatomy; Brain, magnetic resonance

AJNR Am J Neuroradiol 17:23–26, January 1996

Magnetic resonance (MR) imaging has been effective in depicting the hippocampus and in detecting mesial sclerosis in temporal lobe epilepsy (1–11). Routine MR imaging techniques do not clearly distinguish the histologic layers and all the subdivisions of the hippocampus. MR demonstration of the subdivisions and layers of Ammon's horn may improve the diagnosis of mesial temporal sclerosis, because some portions of the hippocampus are more susceptible to hypoxic injury than others. CA1 (Sommer sector) is also known as the vulnerable sector. CA4 (Bratz sector) has been referred to as the medium vulnerability sector. CA2 and CA3 (Spielmeyer sector) have been called the resistant sector (1). We studied the MR appearance of the body of Ammon's horn in the hippocampal formation with high-resolution MR imaging at 3.0 T.

Received March 8, 1995; accepted after revision July 24.

From the Departments of Radiology (L.P.M., V.M.H.) and Pathology (K.-C.H.), the Medical College of Wisconsin (M.J.M.), Milwaukee.

Address reprint requests to Victor M. Haughton, MD, Department of Radiology, Medical College of Wisconsin, Froedtert Memorial Lutheran Hospital, 9200 W Wisconsin Ave, Milwaukee, WI 53266.

AJNR 17:23–26, Jan 1996 0195-6108/96/1701–0023

Materials and Methods

Five brains without neurologic disease obtained from routine autopsy cases were fixed in 10% buffered formalin solution for 3 weeks. A specimen 4 cm in height and 2.5 cm in diameter (with the long axis in the anteroposterior direction) was harvested from each brain by means of gross dissection. The specimens were placed into 45-mL polypropylene containers with sufficient 10% buffered formalin solution to fill the container, and the containers were sealed to exclude air.

The specimens in the containers were imaged in a Biospec 3.0-T 60-cm imager (Bruker, Karlsruhe, Germany) with a 3-cm-diameter solenoid coil (M.J.M., unpublished data, 1994). Spin-echo interleaved images were obtained in coronal planes with a sequence of 1000/30/4 (repetition time/echo time/excitations), a 256 × 256 matrix, 1-mm section thickness, 3- or 4-cm field of view, and a 1-mm gap. Acquisition time was 17 minutes for a series of 11 images.

Two of the specimens were embedded in paraffin and sectioned with a microtome in 6-μm thicknesses at selected intervals. The sections were stained with hematoxylin-eosin and Luxol fast blue and photographed with a 35-mm camera and macro lens. The histologic sections were correlated with the corresponding MR image from the same specimen.

In anatomic sections, white and gray matter structures were identified by location and staining characteristics. The body of the hippocampus was identified in coronal sections as two interlocking U-shaped structures, an upside-down U, which is mostly Ammon's horn, and a smaller, more medial right-side-up U, which is the dentate gyrus and CA4. The following criteria were used to distin-

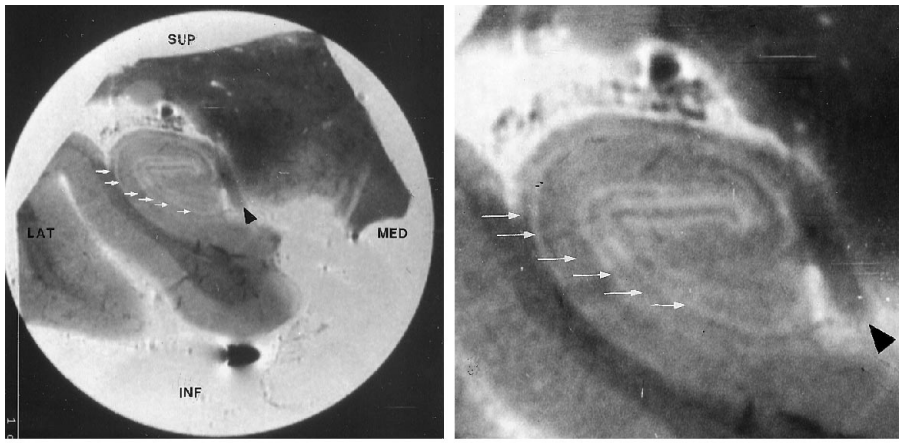

Fig 1. *A*, High-resolution MR image through the body of the hippocampus. The six layers of the hippocampus (*small arrows*) represent, from top to bottom, the alveus, stratum oriens, stratum pyramidale, stratum radiatum, stratum lacunosum, and stratum moleculare. The fimbria (*arrowhead*) is evident. *SUP* = superior, *MED* = medial, *INF* = inferior, and *LAT* = lateral aspects of hippocampus.

B, Magnified image of *A*. Labeling is consistent with that of *A*.

guish the four subdivisions of Ammon's horn (CA1–CA4): CA1 was defined as the lateral arm of Ammon's horn; CA2 was defined as the superior flexure of Ammon's horn between its medial and lateral arms; CA3 was defined as the medial arm of Ammon's horn, which extends into the concavity of CA4 and the dentate gyrus; and CA4 was defined as that portion of Ammon's horn nested within the dentate gyrus. Six layers are differentiated in CA1 by staining characteristics. The six layers are designated, from lateral to medial, the alveus, stratum oriens, stratum pyramidale, stratum radiatum, stratum lacunosum, and stratum moleculare.

Results

In MR images (1000/30), signal intensity is low in white matter tracts, higher in cellular regions, and highest in the cerebrospinal fluid spaces that contain fluid. MR images show six discrete layers of differing thicknesses and varied signal intensities interspersed in the convoluted, upside-down U-shaped body of Ammon's horn (Fig 1). The most peripheral layer is a thin zone of low-intensity signal that represents the alveus, which curves over the outer margin of the lateral and superior aspect of the hippocampus to coalesce medially to form the fimbria. At CA1, MR images show a thin strip of high-intensity signal just medial to the alveus corresponding to the stratum oriens. MR images show a thicker layer with a homogeneous, intermediate signal intensity deep to the stratum oriens consistent with the stratum pyramidale. Medial to the stratum pyramidale is a thin, higher-intensity stripe that corresponds to the stratum radiatum. A thin lower-intensity stripe medial to the stratum radiatum corresponds to the stratum lacunosum.

The four subdivisions of Ammon's horn may be distinguished with coronal MR imaging through the body of the hippocampus (Fig 2). CA1 forms the lateral arm of Ammon's horn. CA2 forms the superior curve of the upside-down U configuration of Ammon's horn near the superior limit of the stratum lucidum, the curvilinear zone of lower signal intensity near strata pyramidale and radiatum. CA3 represents that portion of the medial arm of Ammon's horn between CA2 and the concavity of the dentate gyrus. CA4 is nested within the dentate gyrus.

Discussion

Investigators have described the MR appearance of the hippocampus but not the four subdivisions of Ammon's horn or the six layers of CA1 (1–3, 9–12). Hayes and colleagues (9) using surface-coil phased-array MR imaging, demonstrated improved resolution of the hippocampus in vivo but were unable to resolve the components of Ammon's horn. This article describes the MR appearance of the subdivisions and layers of Ammon's horn.

Our observations may not be directly extrapolated to clinical imaging because experimental imaging parameters different from prevalent clinical imaging techniques were used to optimize resolution. All possible anatomic structures and variations may not have been identified within the samples studied because of normal anatomic variation. Anatomic distortion may have been introduced into our specimens by the method of harvest, through handling of specimens, or by shrinkage through fixation. Finally, the correlation of MR images of 1 mm

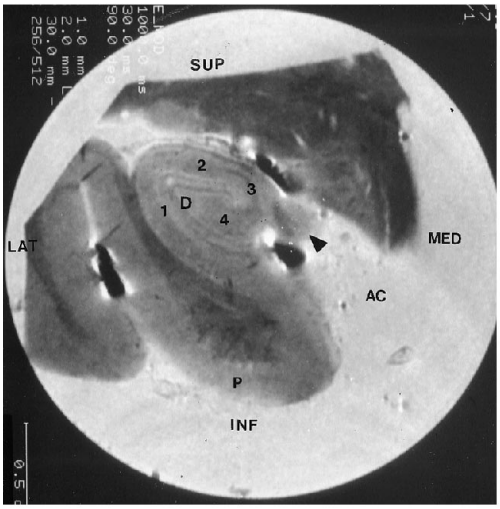

2

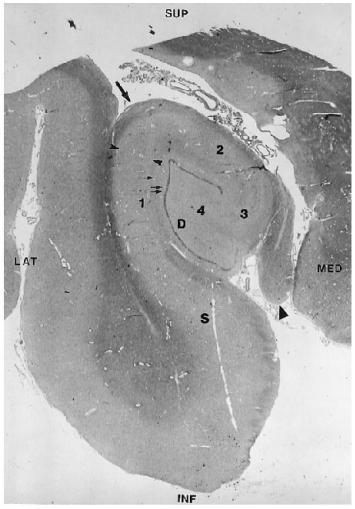

3

Fig 2. High-resolution MR image through the body of the hippocampus 4 mm anterior to Figure 1. The subdivisions of Ammon's horn—CA1 (*1*), CA2 (*2*), CA3 (*3*), and CA4 (*4*)—are identified. The fimbria (*arrowhead*) is evident. The parahippocampal gyrus (*P*), ambient cistern (*AC*), and dentate gyrus (*D*) are identified. *SUP* = superior, *MED* = medial, *INF* = inferior, and *LAT* = lateral aspects of hippocampus.

Fig 3. Coronal anatomic section through the body of the hippocampus corresponding to Fig 1A. The subdivisions of Ammon's horn—CA1 (*1*), CA2 (*2*), CA3 (*3*), and CA4 (*4*)—are evident. The subiculum (*S*) and dentate gyrus (*D*) are identified. The alveus (*large arrow*) curves medially to terminate in the fringelike fimbria (*arrowhead*). The stratum locunosum (*single small arrow*) and stratum moleculare (*double small arrows*) are identified. Gross inspection of the anatomic section cannot distinguish the stratum oriens, stratum pyramidale, and stratum radiatum from one another (the three layers are collectively bounded with *small arrowheads*). Discrimination of these layers on the histologic section was based on cell architecture as studied with a high-powered microscope.

section thickness with 6-μm-thick anatomic sections necessarily would be imperfect.

The separation of CA1–CA4 in Ammon's horn is defined by histologic differences in cell bodies, and the border from one sector to another is actually a gradual transition in the dominant cell type. A good rough correlation exists between our definition of CA1 to CA4, based largely on geographic criteria, and the histologic definition of those sectors (13, 14). The subdivisions of Ammon's horn were identified in all five specimens studied. However, some interspecimen variation in the ability to discriminate the six layers of CA1 was noted. A minimum of four of the six layers of CA1 were identified in each specimen. The distinction between cellular layers was equally well seen throughout the hippocampus in a given specimen.

Resolution in our MR images was increased by small field-of-view imaging at 3.0 T. With our present imaging techniques, the signal-to-noise ratio at 3.0 T exceeds that at 1.5 T by a factor of 1.4. Obtaining these results at 1.5 T would require longer acquisition times. Our results cannot be attributed exclusively to imaging at higher field strength, since MR images have been obtained at 1.5 T that allow discrimination of some of the layers of CA1 (L.P.M., unpublished data, 1991). We obtained our high-resolution images by using a small field of view and a specially designed 3.0-cm-diameter solenoid coil matched to the tissue region. Because the signal-to-noise ratio at a given location within the brain is determined by noise contributed by all the tissue within a coil volume, our signal-to-noise ratio was improved by imaging small tissue specimens in our solenoid coil (9). Although fixation changes signal intensity, whether it improves contrast enough to explain our results is questionable (15–17). The absence of motion artifacts from head movement, brain pulsations, and flow of blood and cerebrospinal fluid also undoubtedly improved our

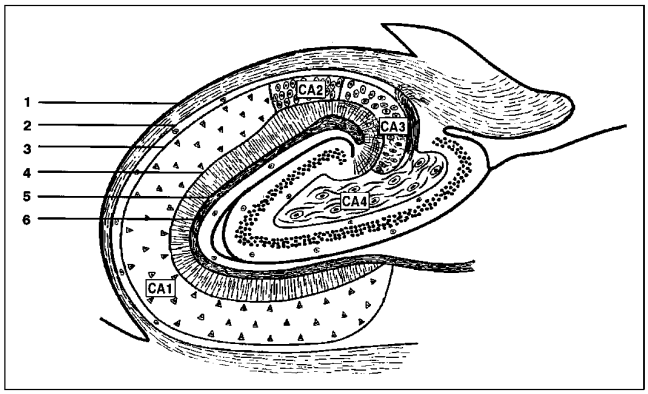

Fig 4. Coronal schematic drawing shows the subdivisions of Ammon's horn and six layers of CA1. The subdivisions of Ammon's horn (CA1–CA4) are identified. The six layers of CA1 are the alveus (*1*), stratum oriens (*2*), stratum pyramidale (*3*), stratum radiatum (*4*), stratum lacunosum (*5*), and stratum moleculare (*6*).

resolution. To achieve this resolution clinically, we need to design strategies to get a small field of view with better signal-to-noise ratio for the temporal lobe. With MR techniques that achieve sufficient resolution differential, sclerosis of CA1 and CA3 of Ammon's horn may be resolved.

We experimented with a variety of imaging protocols to best resolve the six layers of CA1. Spin-echo images with parameters of 4000/40–80/4, 2000/20–40/4, 1500/60/4, and 376/19/4 failed to discriminate the layers of CA1, as with the 1000/30/4 sequence.

In summary, MR imaging can distinguish the six layers of CA1 by location, course, signal intensity, and thickness. The four subdivisions of Ammon's horn can be distinguished by location and by the layers that compose them. This study suggests the higher-resolution MR imaging techniques may have application in the evaluation of both temporal lobe epilepsy and hypoxic states, including carbon monoxide poisoning, drowning, and sickle-cell anemia.

Acknowledgements

We thank Richard Johnson of the Department of Biophysics at the Medical College of Wisconsin for his assistance in constructing the solenoid coil used in this study. We also thank Chad Moritz, also of the Department of Biophysics, for his help in acquiring the MR images used for this article.

References

1. Mark LP, Daniels DL, Naldich TP, Yetkin Z, Borne JA. The Hippocampus. *AJNR Am J Neuroradiol* 1993;14:709–712
2. Watson C, Andermann F, Gloor P, et al. Anatomic basis of amygdaloid and hippocampal volume measurement by magnetic resonance imaging. *Neurology* 1992;42:1743–1750
3. Jack CR, Bently MD, Twomey CK, Zinsmeister AR. MR imaging-based volume measurements of the hippocampal formation and anterior temporal lobe: validation studies. *Radiology* 1990;176:205–209
4. Naidich TP, Daniels DL, Haughton VM, Williams A, Pojunas K, Palacios E. Hippocampal formation and related structures of the limbic lobe, anatomic-MR correlation, I: surface features and coronal sections. *Radiology* 1987;162:747–754
5. Naidich TP, Daniels DL, Haughton VM, Williams A, Pojunas K, Palacios E. Hippocampal formation and related structures of the limbic lobe, anatomic-MR correlation, II: sagittal sections. *Radiology* 1987;162:755–761
6. Jack CR, Sharbrough FW, Twomey CK, et al. Temporal lobe seizures: lateralization with MR volume measurements of the hippocampal formation. *Radiology* 1990;175:423–429
7. Jack CR, Sharbrough FW, Marsh WR. Use of MR imaging for quantitative evaluation of resection for temporal lobe epilepsy. *Radiology* 1988;169:463–468
8. Jack CR, Twomey CK, Zinsmeister AR, Sharbrough FW, Peterson RC, Cascino GC. Anterior temporal lobes and hippocampal formations: normative value measurements for MR images in young adults. *Radiology* 1989;172:549–554
9. Hayes CE, Tsuruda JS, Mathis CM. Temporal lobes: surface MR coil phased-array imaging. *Radiology* 1993;189:918–920
10. Bronen RA, Cheung G. MRI of the normal hippocampus. *Magn Reson Imag* 1991;9:497–500
11. Bronen RA, Cheung G. Relationship of the hippocampus and amygdala to coronal MRI landmarks. *Magn Reson Imaging* 1991;9:449–457
12. Bronen RA. Hippocampal and limbic terminology. *AJNR Am J Neuroradiol* 1992;13:943–945
13. de No R Lorente. Studies on the structure of the cerebral cortex: I. the area entorhinalis. *J Psychol Neurol* 1933;45:381–438
14. de No R Lorente. Studies on the structure of the cerebral cortex: II. continuation of the study of the ammonic system. *J Psychol Neurol* 1934;46:113–177
15. Unger EC, Gado MH, Fulling KF, Littlefield JF. Acute cerebral infraction in monkeys; an experimental study using MR imaging. *Radiology* 1987;162:789–795
16. Kamman RL, Go KG, Stomp GP, Hulstaert CE, Berendsen HJC. Changes of relaxation times T1 and T2 after biopsy and fixation. *Magn Reson Imaging* 1985;3:245–250
17. Thickman DL, Kundel HL, Wolf G. Nuclear magnetic resonance characteristics of fresh and fixed tissue: the effect of elapsed time. *Radiology* 1983;148:183–185